J. Chem. Sci. Vol. 127, No. 3, March 2015, pp. 509–518.
DOI 10.1007/s12039-015-0802-5

Structural and optical properties of zinc titanates synthesized by precipitation method

LOKESH BUDIGI[a], MADHUSUDHANA RAO NASINA[a,*], KALEEMULLA SHAIK[a] and SIVAKUMAR AMARAVADI[b]

[a]Thin Films Laboratory, Materials Physics Division, School of Advanced Sciences, VIT University, Vellore 632 014, Tamil Nadu, India
[b]School of Advanced Sciences, VIT University, Vellore 632 014, Tamil Nadu, India
e-mail: drnmrao@gmail.com

MS received 8 June 2014; revised 30 August 2014; accepted 18 September 2014

Abstract. Synthesis of zinc titanates was carried out using a simple precipitation method followed by calcination at different temperatures to obtain different phases of the material. The phase transition characteristics, presence of functional groups, structural aspects and optical bandgaps with respect to calcination temperature were studied by thermal analysis, EDAX, FT-IR, powder XRD, Raman and UV-Vis spectroscopy respectively. The compound on heat treatment at 100°C for 24 h showed broadened peaks in XRD. With increasing temperature of calcination, the compound appeared to turn to crystalline phase and cubic $ZnTiO_3$ phase was observed at 600°C. Partial phase transformation of cubic phase $ZnTiO_3$ into hexagonal ilmenite type $ZnTiO_3$ was observed in the temperature range 700°C to 900°C. At 1000°C both cubic and hexagonal ilmenite phases decomposed into cubic phase Zn_2TiO_4 and rutile TiO_2. FT-IR showed M-O bonds in the range of 400 cm^{-1} to 700 cm^{-1}. Raman spectra of cubic defect spinel $ZnTiO_3$ and cubic inverse spinel Zn_2TiO_4 were found to be similar. The optical bandgap calculated using diffuse reflectance spectra was found to be in the range of 3.59 to 3.84 eV depending on calcination temperature.

Keywords. Zinc titanate; phase transition; Raman spectroscopy; bandgap; diffuse reflectance spectroscopy.

1. Introduction

Zinc titanate metal oxides have attracted considerable attention for use as sorbent for desulfurization of coal gas,[1] catalyst in liquid phase organic transformations,[2] dielectric and microwave resonators,[3] gas sensors,[4] oxidation of hydrocarbons or CO and NO reduction,[5] semiconductor material,[6] photocatalytic material,[7] and also in paints as pigments.[8] Owing to these properties, several methods have been employed for the synthesis of zinc titanates such as solid state reaction,[9–11] sol-gel,[12–14] Pechini process,[15] hydrothermal method,[16] sputtering,[17,18] microwave heating,[19] and molten salt method,[20] etc. In solid-state reactions, formation of end product depends on the calcination temperature, particle size and crystalline phase of starting materials TiO_2 and ZnO. Liu *et al.*[21] proposed that the formation of Zn_2TiO_4 and $Zn_2Ti_3O_8$ are confined to the presence of anatase TiO_2, while $ZnTiO_3$ will be formed only in the presence of rutile TiO_2 due to structural similarities. On the other hand Zn_2TiO_4 could be synthesized by solid state reaction using ZnO and TiO_2 in 2:1 molar ratio, while $ZnTiO_3$ could not be synthesized with 1:1 molar ratio of ZnO and TiO_2 due to the narrow phase stability temperature region of $ZnTiO_3$, decomposing it into Zn_2TiO_4 and rutile TiO_2.[22] Thus making single phase $ZnTiO_3$ by solid state reaction is difficult. Metal alkoxides are generally used as starting materials in sol-gel synthesis of zinc titanates. Metal alkoxides are moisture sensitive and are easily hydrolysed to form metal hydroxides and their respective alcohols. Sol-gel or microwave assisted sol-gel method requires controlled hydrolysis of metal alkoxides in anhydrous alcohol to get uniform particle size distribution.[12–14] Further, in sol-gel synthesis there was no consensus on the product obtained at low temperature (<700°C). Though the starting reagents were taken in 1:1 molar ratio, $Zn_2Ti_3O_8$ was reported as a low temperature form of zinc titanates without accounting for the possible existence of ZnO to balance the stoichiometry.[14,16] Studies by Mrazek *et al.*[12] have not confirmed the existence of $Zn_2Ti_3O_8$ which on calcination at higher temperatures transforms into $ZnTiO_3$. Thus there is a need to study zinc titanate formation at low temperature. In Pichini process, metal ions were reacted with citric acid ligand to form citric acid metal complexes. These citric acid

*For correspondence

metal complexes were then converted to thick gel by heating around 90°C and later combusted to form metal oxides. Finally the combusted products were calcined at high temperature to obtain phase transformation.[15] Hydrothermal synthesis requires special hydrothermal setup to maintain optimum temperature and pressure.[16] In sputtering techniques, zinc titanates synthesized by solid state reactions are generally used as targets for thin film coating on various substrates.[17,18] In molten salt synthesis, ratio of molten salt to oxides is maintained to be very high. After completion of the reaction, final products are obtained by removing molten salts by repeated washing with distilled water.[20] Compared to the methods mentioned in this paper, precipitation method adopted in this study has a number of advantages such as ease of handling reagents, and zero requirement of special apparatus or solvents. Precipitation reactions can be performed in aqueous media. Apart from maintaining pH to ensure optimum precipitation of both Zn and Ti, no special experimental conditions are required.

The main aim of the present study is to synthesize zinc titanates by a simple precipitation method and to study the phase transitions by various characterization techniques, to investigate phase transformation to predict formation of zinc titanium hydroxide $ZnTi(OH)_6$ and to study the low temperature phase of zinc titanates acting as precursors for formation of zinc titanium oxides.

2. Experimental

2.1 *Materials and methods*

Anhydrous $ZnCl_2$ powder (99.995%, Sigma Aldrich), $TiCl_3$ solution ($TiCl_3$ minimum 12% in HCl solution, Sigma Aldrich) and NaOH (98.5%, Sigma Aldrich) were used as starting materials for zinc titanate synthesis. To maintain stoichiometry the amount of Ti present in $TiCl_3$ in 12% HCl solution was gravimetrically estimated from the quantity of TiO_2 formed.[23] 50 mL of 0.1 mole aqueous $ZnCl_2$ solution and 50 mL of 0.1 mole $TiCl_3$ in HCl solution were mixed together to form a violet coloured solution measuring pH 1.43. To this solution, 1 M NaOH solution was added dropwise till pH reached 7.0. A dark blue coloured zinc titanium hydroxide precipitate was formed instantaneously. Cassaignon *et al.*[23] reported that $TiCl_3$ aqueous solution on reacting with NaOH solution at pH > 4.5 forms air unstable partially oxidized dark blue $Ti(OH)_{3+x}$ precipitate where x is a fraction indicating the rate of oxidation, and turns white after several hours due to oxidation in atmospheric oxygen. Similarly the dark blue coloured zinc titanium hydroxide precipitate was oxidized by stirring in presence of atmospheric oxygen for 24 h to form white zinc titanium hydroxide precipitate. This precipitate was washed several times with distilled water and filtered using a suction pump. Filtrate was tested qualitatively for Zn^{2+}, Ti^{3+} and Ti^{4+} ions as per procedure available.[24] Absence of Zn^{2+}, Ti^{3+} and Ti^{4+} in the filtrate solution confirmed the complete precipitation of metal ions as hydroxides. The precipitate was dried at 100°C for 24 h, ground to result in soft precursor powders and calcinated in a silicon carbide furnace at a heating rate of 4°C/min in the temperature range 100°C to 1000°C for 2 h each and gradually cooled to room temperature to form zinc titanates of different phases.

2.2 *Characterization*

TGA-DTA experiments were carried out using SDT Q600 V20.9 instrument in DSC-TGA standard module in nitrogen atmosphere at a gas flow rate of 100 mL/min at a heating rate of 4°C/min using 18 mg of the precursor sample to understand the changes in composition. The thermal analysis was carried from room temperature to 600°C, using alumina cups as sample holders and alumina powder as reference. Elemental analyses of the samples were carried out using FEI Quanta FEG 250 Scanning Electron Microscope (SEM) equipped with EDAX Apollo X for energy dispersive X-ray spectroscopy. The crystalline structure of the samples was determined by powder XRD using BRUKER D8 Advance X-ray diffractometer using CuK_α radiation (λ =0.15406 nm). The diffraction pattern was recorded with scanning rate of 2°/min and step size of 0.02° ranging from 10° to 80°. FT-IR spectra were recorded using KBr pellet method on Shimadzu IR affinity spectrophotometer in the range from 4000 cm^{-1} to 400 cm^{-1}. Raman spectra were recorded with LABRAM HR 800 micro Raman spectrometer with a laser excitation wavelength of 633 nm laser. UV-Vis spectra were recorded in diffuse reflectance mode (R) on a JASCO UV-Vis NIR V670 spectrophotometer, using $BaSO_4$ as reference.

3. Results and Discussion

3.1 *Thermal analysis*

TGA and DTA curves of the precursor powders heated in nitrogen atmosphere at a rate of 4°C/min using alumina powder as the reference are shown in the figure 1. During precipitation, synthesis, zinc and titanium hydroxides were observed to have formed as shown in equations 1 and 2. From the thermal analysis,

the observed weight loss could be attributed only to loss of water through thermal decomposition of hydroxide groups and formation of oxide products from the tentative $ZnTi(OH)_6$ hydroxides as shown in equations 3 and 4. A total weight loss of 27.83% was observed when the temperature was increased from RT to 250°C which is in agreement with the theoretical weight loss of 25.10% due to formation of amorphous $Zn_2Ti_3O_8$ and ZnO as can be anticipated from equation 3.

$$ZnCl_2 + TiCl_3 + 5\,NaOH \longrightarrow Zn(OH)_2\downarrow + Ti(OH)_{3+x}\downarrow + 5\,NaCl \quad x = \text{fraction indicating rate of oxidation.} \tag{1}$$

$$Zn(OH)_2\downarrow + Ti(OH)_{3+x}\downarrow \xrightarrow{\text{oxidation in presence of atmospheric oxygen}} ZnTi(OH)_6\downarrow \tag{2}$$

$$3\,ZnTi(OH)_6 \xrightarrow{-9H_2O} Zn_2Ti_3O_8 + ZnO \tag{3}$$

$$Zn_2Ti_3O_8 + ZnO \longrightarrow 3\,ZnTiO_3 \tag{4}$$

EDAX spectra of the uncalcined zinc titanium hydroxide (figure 2a) shows that Zn, Ti and O are present in 30.97, 22.32 and 46.71% and samples calcined at 600°C (figure 2b) showed 40.45, 28.72 and 30.83% as atomic percentages which correspond to the empirical formulae $ZnTiO_6$ and $ZnTiO_3$, respectively while hydrogen was not detected because of lower atomic mass (EDAX can detect elements only from carbon onwards). From the method adopted it is apparent that hydroxides are expected and the empirical formula $ZnTiO_6$ obtained from EDAX may be due to the tentative zinc titanium hydroxide $ZnTi(OH)_6$. This result is similar to the dehydration of $CuSn(OH)_6$ and other $AB(OH)_6$ hydroxides to form $CuSnO_3$ and ABO_3 oxides as described by Zhong *et al*.,[25] and Chamberland and Silverman.[26] A weight loss of 2.73% was observed during the crystallization and formation of cubic $ZnTiO_3$ from amorphous $Zn_2Ti_3O_8$ and ZnO in the temperature range of 250°C to 600°C. Two endothermic peaks observed at 220°C and 320°C can be attributed to the partial decomposition of $ZnTi(OH)_6$ precursor to anatase TiO_2 and ZnO as seen in XRD patterns of samples calcined at 200°C and 300°C respectively. This result is similar to the decomposition of $CuSn(OH)_6$, $ZnSn(OH)_6$ and $CdSn(OH)_6$ and formation of amorphous $CuSnO_3$, $ZnSnO_3$ and $CdSnO_3$ respectively.[26–28] An exothermic peak was observed at 415°C indicating the formation of amorphous zinc titanate which crystallized to $Zn_2Ti_3O_8$ at 500°C as observed in the powder XRD pattern.

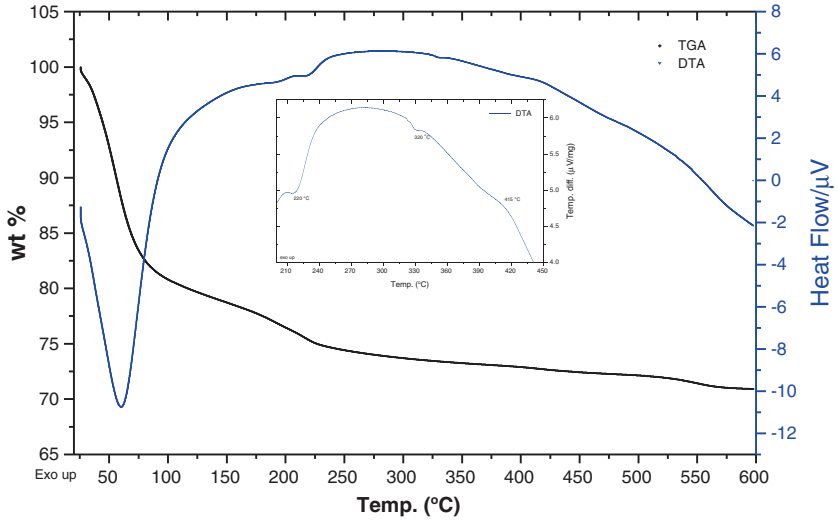

Figure 1. TGA-DTA curves of as synthesized zinc titanate powders.

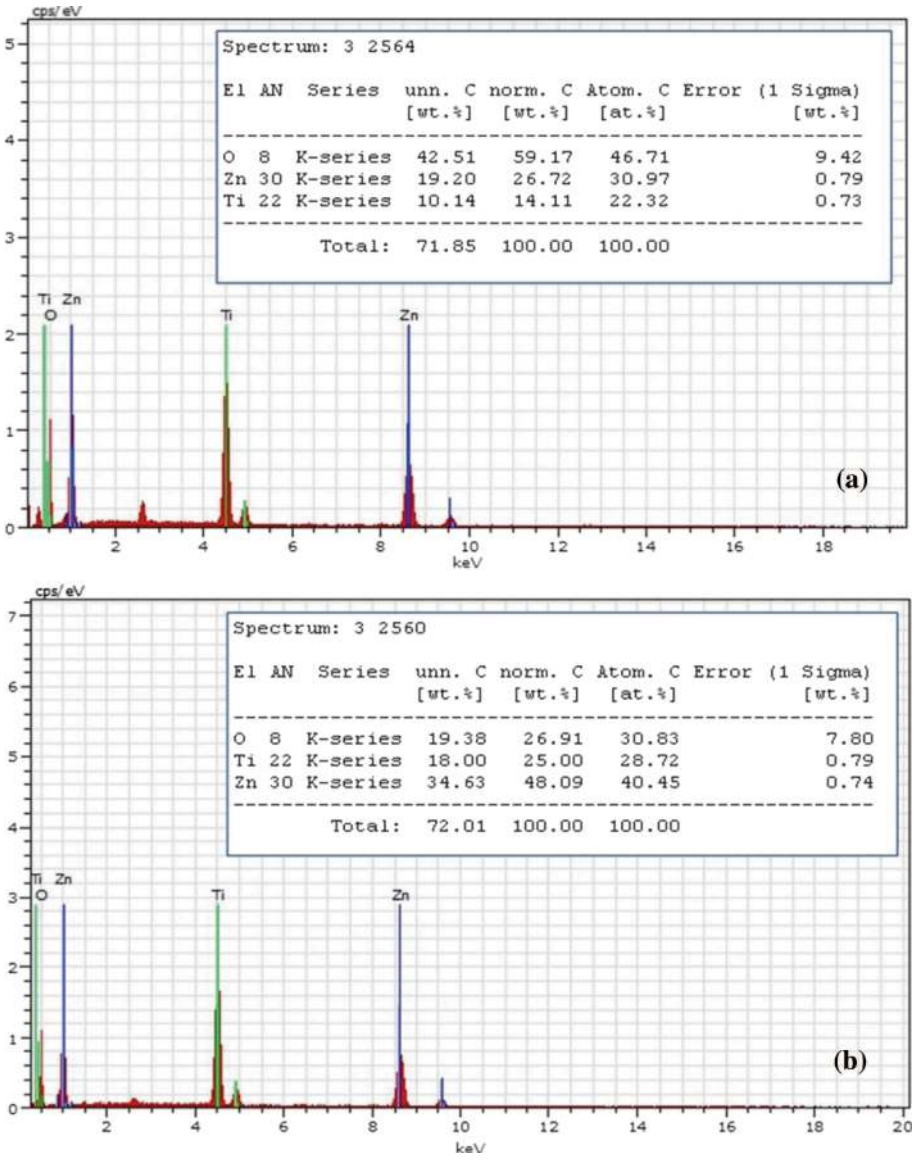

Figure 2. EDAX spectra of, (**a**) uncalcined zinc titanium hydroxide and (**b**) calcined at 600°C/2h. Inset: EDAX elemental composition.

3.2 *Powder XRD*

XRD pattern of the as-synthesized precursor powder indicates that the sample is amorphous with two broad peaks at 2θ ~32° and ~60°. Neither ZnO nor TiO_2 phases were observed (figure 3a). It was observed that during synthesis of ZnO and TiO_2 from $ZnCl_2$ and $TiCl_3$ separately under identical conditions ZnO were found to be crystalline at room temperature, while TiO_2 crystallized on calcination.[23] Absence of ZnO in the as-synthesized sample powders and absence of Zn^{2+}, Ti^{3+} or Ti^{4+} in the filtrate suggests that Zn and Ti taken in 1:1 mole ratio were completely precipitated to form a tentative $ZnTi(OH)_6$ or $ZnTiO_3.3H_2O$ type ternary metal oxide precursor. On heating them at 100°C for 24 h, a crystalline phase with three broad XRD peaks at 2θ 29.10°, 48.05° and 57.05° is seen to have formed (figure 3b). To the best of our knowledge no crystalline phase was reported so far in zinc titanate system at temperatures as low as 100°C. Further investigation is needed to identify the precise crystal structure of the newly formed crystalline phase. On further calcination at 200°C for 2 h, an amorphous phase is seen to have formed (figure 3c). This is comparable with the decomposition of crystalline $CuSn(OH)_6$ and $BaSn(OH)_6$ in to amorphous phases which on subsequent calcination at higher temperatures crystallize to $CuSnO_3$ and $BaSnO_3$ respectively.[25,29] Similarly, Chamberland and Silverman reported the formation of ABO_3 products from $AB(OH)_6$ derivatives where A is an alkaline earth metal and B is either Sn or Ir or Os or Pt.[26] On increasing the calcination temperature to 300°C

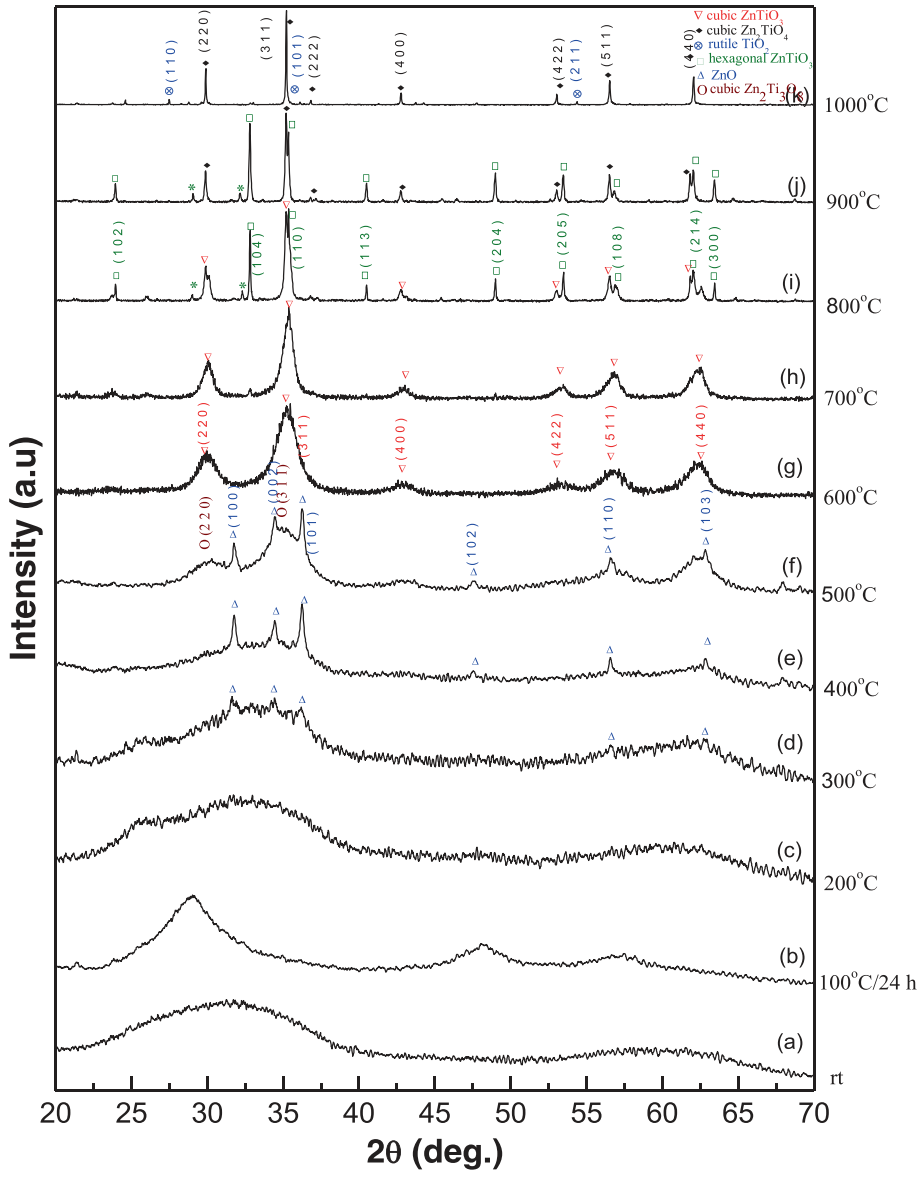

Figure 3. Powder XRD pattern of assynthesized and samples calcined at different temperatures, each for 2 h.

(figure 3d) three low intensity peaks corresponding to (1 0 0), (0 0 2) and (1 0 1) planes of ZnO were observed and their intensity increased on calcination at 400°C (figure 3e) indicating crystallization of ZnO. On calcination at 500°C for 2 h (figure 3f) (2 2 0), (3 1 1) and (4 0 0) peaks of cubic phase $Zn_2Ti_3O_8$ appeared along with ZnO. $Zn_2Ti_3O_8$ is a thermodynamically stable compound having defect spinel structure represented as $Zn_{2-x}\square_x[Zn_x\square_{1-x}Ti_3]O_8$where $0\leq x\leq 1$(symbol □ represents unoccupied sites).[9,30] Here it could be noted that during wet chemical synthesis of zinc titanates, though starting materials Zn and Ti cations were taken in 1:1 mole ratio, the crystalline phase observed around 500°C to 600°C was considered as cubic phase $Zn_2Ti_3O_8$ in which Zn and Ti were in 2:3 mole ratio without accounting for another 1 mole of Zn.[13,16,31,32] Solubility of ZnO in $Zn_2Ti_3O_8$ is not reported in literature.[9,30] It is difficult to differentiate cubic phase $ZnTiO_3$ and cubic phase $Zn_2Ti_3O_8$ because they have similar crystal structure and lattice parameters.[11] In samples calcined at 500°C the possibility of cubic phase $ZnTiO_3$ can be ruled out by the presence of ZnO. At 600°C (figure 3g) ZnO and cubic phase $Zn_2Ti_3O_8$ undergo solid state reaction to form cubic phase $ZnTiO_3$. On increasing the calcination temperature from 600°C to 700°C (figure 3h) crystallinity of cubic phase $ZnTiO_3$ increases as evidenced from the increased intensities of (2 2 0) peak at 30.45° and (3 1 1) peak at 35.37°. At 700°C, (1 0 4) peak appeared at 2θ of 32.82° indicating the formation of hexagonal ilmenite phase $ZnTiO_3$ (figure 3h). Further at 800°C (figure 3i) (3 1 1) peak of cubic $ZnTiO_3$ split into two peaks corresponding to the (3 1 1) and

(1 1 0) peaks of cubic $ZnTiO_3$ and hexagonal ilmenite $ZnTiO_3$ respectively and their intensities were seen to increase on calcination till 900°C (figure 3j). This indicates the partial phase transformation of cubic phase $ZnTiO_3$ to hexagonal ilmenite $ZnTiO_3$ and their coexistence in the temperature range of 700°C to 900°C. In the calcination temperature range 700°C to 900°C, it is difficult to distinguish between cubic $ZnTiO_3$, hexagonal ilmenite $ZnTiO_3$ and cubic Zn_2TiO_4 because the cubic phase $ZnTiO_3$ (3 1 1) and (2 2 0) peaks, the cubic phase Zn_2TiO_4 (3 1 1) and (2 2 0) peaks and hexagonal (1 1 0) peaks appear in a narrow 2θ range and overlap each other.[11] At 1000°C (figure 3k) both cubic and hexagonal ilmenite phase $ZnTiO_3$ is completely decomposed to cubic Zn_2TiO_4 and rutile TiO_2. The overall sequence of crystallization of zinc titanates and phase evolution with respect to calcination temperature can be tentatively represented as follows:

$$3\ ZnTi(OH)_6 \xrightarrow{< 400\ ^oC} Zn_2Ti_3O_8\ (amorphous) + ZnO \quad (5)$$

$$Zn_2Ti_3O_8\ (amorphous) + ZnO \xrightarrow{400\ ^oC - 500\ ^oC} Zn_2Ti_3O_8\ (cubic) + ZnO \quad (6)$$

$$Zn_2Ti_3O_8\ (cubic) + ZnO \xrightarrow{600\ ^oC - 700\ ^oC} 3\ ZnTiO_3\ (cubic) \quad (7)$$

$$3\ ZnTiO_3\ (cubic) \xrightarrow{700\ ^oC - 900\ ^oC} 2\ ZnTiO_3\ (cubic) + ZnTiO_3\ (hexagonal) \quad (8)$$

$$2\ ZnTiO_3\ (cubic) + ZnTiO_3\ (hexagonal) \xrightarrow{> 900\ ^oC} 1.5\ Zn_2TiO_4\ (cubic) + 1.5\ TiO_2\ (rutile) \quad (9)$$

3.3 *FT-IR spectra*

FT-IR spectra of the zinc titanates are as shown in the figure 4. As-synthesized samples dried at 100°C for 24 h exhibited a broad peak at ∼3434 cm^{-1} corresponding to the O-H stretching and a small sharp peak at ∼1631 cm^{-1} are H-O-H bending mode vibrations of the adsorbed water molecules. The bands at ∼2361 cm^{-1} were due to asymmetric stretching of CO_2 from the atmospheric air. The symmetric and asymmetric stretching of C-O bonds were observed at ∼1080 cm^{-1} and ∼1040 cm^{-1} respectively.[33,34] The intensities of O-H stretching (∼3434 cm^{-1}), H-O-H bending (∼1631 cm^{-1}) and the symmetric (∼1080 cm^{-1}) and asymmetric (∼1040 cm^{-1}) C-O bands were seen to reduce gradually with increasing calcination temperature and completely disappear ∼700°C indicating the complete dehydration of the zinc titanate precursors $ZnTi(OH)_6$ or $ZnTiO_3.3H_2O$ to form $ZnTiO_3$ as confirmed from the XRD patterns. With an increase in calcination temperature, the intensities of the characteristic vibrations of TiO_6 octahedra between 400 cm^{-1} and 700 cm^{-1} becomes stronger.[35] The peaks at ∼640 cm^{-1} and ∼530 cm^{-1} may be due to Ti-O stretching vibrations,[24] peaks at ∼619 cm^{-1} and ∼432 cm^{-1} corresponding to the stretching vibrations for the Ti-O and Zn-O bonds.[2] A characteristic band at 735 cm^{-1} appeared at 600°C, and its absorbance is seen to increase rapidly up to 800°C and then decrease gradually till 1000°C. This can be assigned to the Zn-O-Ti bond structure in cubic $ZnTiO_3$ which is formed at 600°C, remains as a major phase up to 800°C and disappears gradually due to decomposition in to Zn_2TiO_4 and TiO_2 at 1000°C as observed from the respective XRD patterns.

3.4 *Raman spectroscopy*

The Raman spectra of zinc titanates calcined at 100°C, 200°C and 400°C are shown in figure 5. No Raman peaks corresponding to neither ZnO nor TiO_2 were observed in samples calcined at 100°C and 200°C. In samples calcined at 400°C, Raman peaks were observed at 437 cm^{-1} and 581 cm^{-1} corresponding to the E_2 and E_1 modes of ZnO[36] (figure 5c) which is consistent with ZnO phase observed in the XRD pattern (figure 3e).

The Raman spectra of zinc titanates calcined at 600, 800 and 1000°C are shown in figure 6. In 800°C calcined sample (figure 6b), Raman peaks corresponding to hexagonal ilmenite $ZnTiO_3$ were observed at 263 cm^{-1}[ν_4(LO)], 341 cm^{-1} [ν_2(LO,TO)], 530 cm^{-1} [ν_1(TO)] and 709 cm^{-1} [ν_1(LO)] along with cubic $ZnTiO_3$.[13] Raman peaks at 260 cm^{-1} (F_{2g}), 306 cm^{-1} (E_g), 342 cm^{-1} (F_{2g}) and 733 cm^{-1} (A_{1g}) modes were assigned to cubic Zn_2TiO_4[37] and peaks observed at

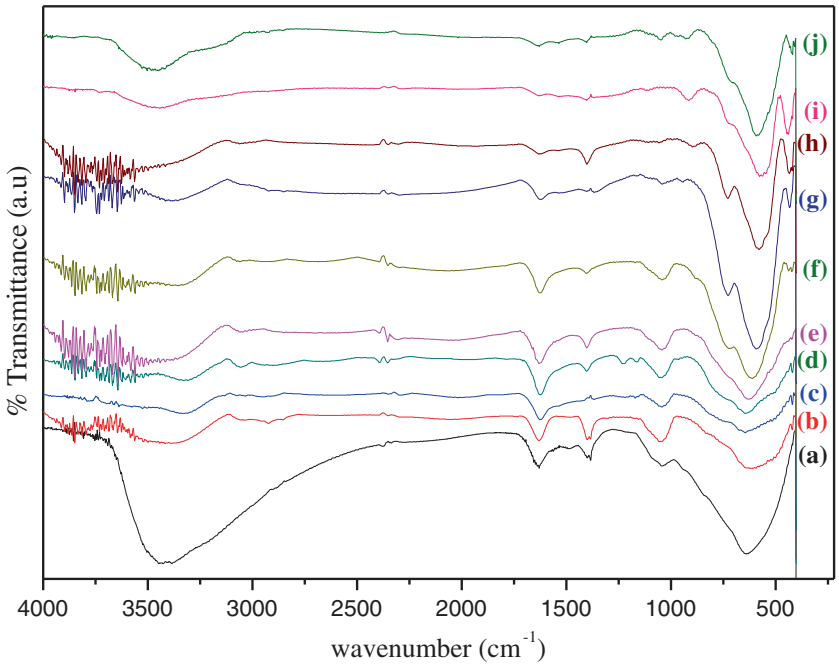

Figure 4. FT-IR spectra of the zinc titanate calcined at (a) 100°C/24 h, (b) 200°C, (c) 300°C, (d) 400°C, (e) 500°C, (f) 600°C; (g) 700°C, (h) 800°C, (i) 900°C, and (j) 1000°C for 2 h each.

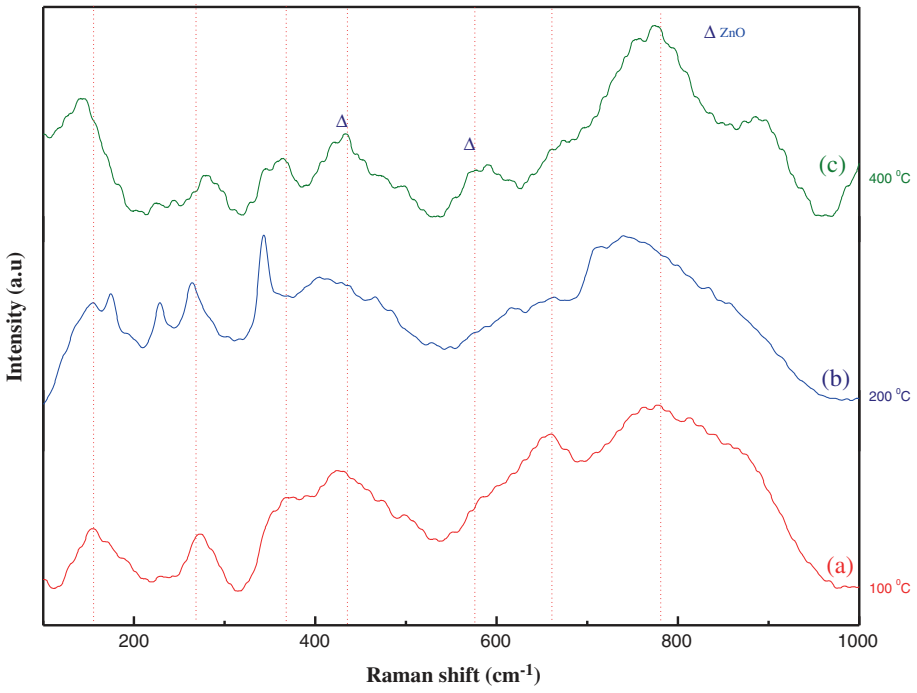

Figure 5. Raman Spectra of zinc titanate powders treated at (a) 100°C/24 h, (b) 200°C/2 h, and (c) 400°C/2 h.

143 cm^{-1} (B_{1g}), 441 cm^{-1} (E_g), 610 cm^{-1} (A_{1g}) and 826 cm^{-1} (B_{2g}) were assigned to rutile TiO_2 formed in samples calcinated at 1000°C.[13,38] XRD patterns of the samples taken at these temperatures confirm the presence of cubic $ZnTiO_3$, hexagonal ilmenite $ZnTiO_3$, cubic Zn_2TiO_4 and rutile TiO_2 lattices. Raman peaks of the samples calcined at 600°C and 1000°C were similar.

The similarity observed in the Raman spectra of the samples calcined at 600°C and 1000°C can be explained based on the similarity in crystal structures of cubic $ZnTiO_3$ and cubic Zn_2TiO_4. Cubic $ZnTiO_3$ has a

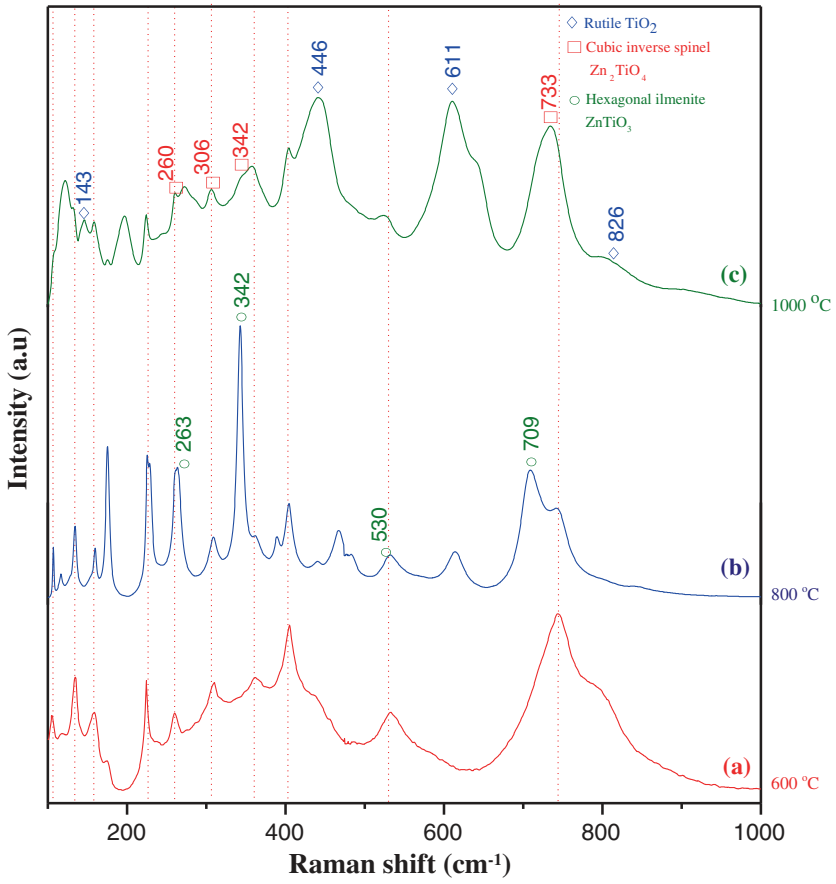

Figure 6. Raman Spectra of zinc titanate powders calcined at (a) 600°C/2h, (b) 800°C/2h, and (c) 1000°C/2h.

defect spinel structure composed of 56 sites represented as $(Zn_8)^t(Zn_{8/3}\square_{8/3}\ Ti_{32/3})°O_{32}$, where 8 Zn^{2+} cations occupy tetrahedral site, while other 8/3 Zn cations along with 32/3 Ti^{4+} cations occupy octahedral sites and the remaining 8/3 octahedral cation sites are vacant. Similarly cubic inverse spinel Zn_2TiO_4 is also composed of 56 sites represented as $(Zn_8)^t(Zn_8\ Ti_8)°O_{32}$, where 8 Zn^{2+} cations occupy tetrahedral sites, while other 8 Zn^{2+} cations along with 8 Ti^{4+} cations occupy the octahedral sites.[12] Both cubic $ZnTiO_3$ and cubic Zn_2TiO_4 have similar crystal structure and lattice parameters.[11] From this it can be inferred that the similarity in the Raman peaks as shown in figure 6 may be due to the similarity in the crystal structure and lattice parameters of cubic defect spinel $ZnTiO_3$ and cubic inverse spinel Zn_2TiO_4.

3.5 *Optical studies*

Figure 7 shows the diffuse reflectance spectra of zinc titanates calcined at different temperatures recorded in the range of 200 to 800 nm using pressed $BaSO_4$ powder as reference. For calculating bandgap of semiconducting metal oxides, the relation between the absorption edge and photon energy ($h\nu$) can be written as $(\alpha h\nu)^n = A(h\nu\text{-}E_g)$, where A is absorption constant, $n = 2$ for direct bandgap and 1/2 for indirect bandgap.[18] To the best of our knowledge, bandgap variation in zinc titanates with respect to crystallite size is not yet reported in literature. Metal oxides like ZnO or SnO_2 show a gradual decrease of bandgap energy with increase in calcination temperature and crystallite size.[39,40] From the figure 7 inset it can be observed that bandgap energies of zinc titanates initially decrease, later increase and finally decrease in the temperature ranges 100 to 300°C, 300 to 800°C and 800 to 1000°C, respectively. Significant phase transformations were observed from the XRD patterns of the samples calcined at the above mentioned temperature ranges. Samples calcined in the temperature range 100 to 300°C were found to be amorphous and showed a red shift of the absorption edge from 336 nm to 345 nm and bandgap decreased from 3.69 eV to 3.59 eV. In the temperature range of 300°C to 800°C ZnO and amorphous zinc titanate phases reacted to form cubic phase $ZnTiO_3$ and showed a gradual blue shift in the absorption edge from 345 nm to 323 nm and the bandgap increased from 3.59 eV to 3.84 eV. The increase in bandgap may be due

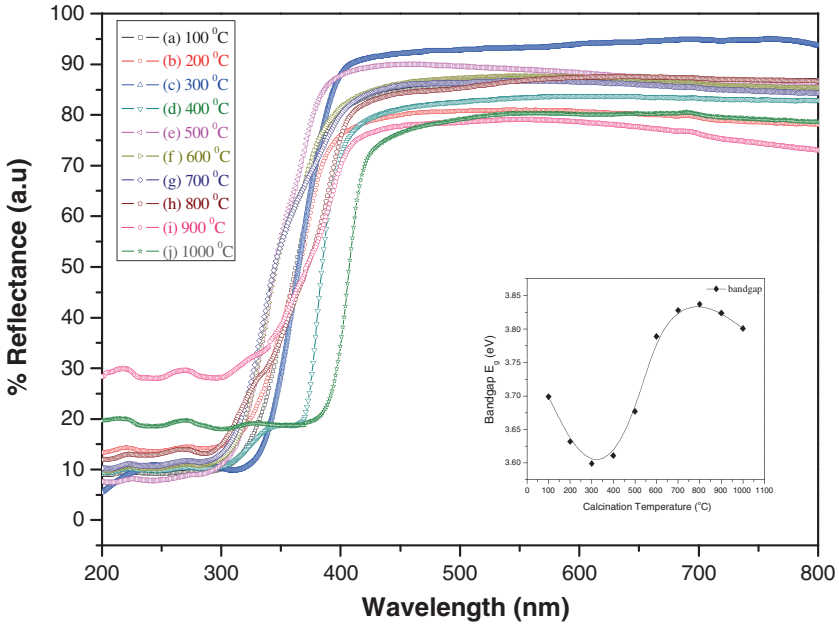

Figure 7. Diffuse reflectance spectra of zinc titanate calcinated at various temperatures. Inset: plot of bandgap (eV) versus calcination temperature (°C).

to the formation and crystallization of $ZnTiO_3$ in the temperature range 300°C to 800°C. Similarly in the calcination temperature range 800 to 1000°C, hexagonal ilmenite phase $ZnTiO_3$ was formed along with cubic phase $ZnTiO_3$ and finally both phases decomposed to form cubic Zn_2TiO_4 and rutile TiO_2. Hexagonal $ZnTiO_3$ and cubic Zn_2TiO_4 have a lower bandgap than the cubic $ZnTiO_3$.[10] Decrease in bandgap from 3.84 eV to 3.80 eV in the temperature range of 800°C to 1000°C may be due to the gradual phase transition from cubic $ZnTiO_3$ to hexagonal $ZnTiO_3$ and final decomposition to Zn_2TiO_4 and rutile TiO_2.

4. Conclusions

Zinc titanate powders were successfully synthesized from $ZnCl_2$ and $TiCl_3$ by a simple precipitation method followed by calcination. From the thermal analysis a total of 27.83% weight loss observed from the tentative $ZnTi(OH)_6$ hydroxide or $ZnTiO_3.3H_2O$ precursor is in good agreement with the theoretical weight loss of 25.10% due to loss of water molecules from $ZnTi(OH)_6$ to form $ZnTiO_3$. A new crystalline phase with three broad peaks was observed in samples calcined at 100°C/24 h. $Zn_2Ti_3O_8$ was observed along with ZnO at 500°C. Crystalline pure cubic phase $ZnTiO_3$ was formed at 600°C. Partial phase transition of cubic $ZnTiO_3$ to hexagonal ilmenite type $ZnTiO_3$ was observed in the temperature range of 700–900°C. Both cubic and hexagonal ilmenite type $ZnTiO_3$ underwent complete decomposition to cubic Zn_2TiO_4 and rutile TiO_2 at 1000°C. The similarity in the Raman spectra of samples calcined at 600°C and 1000°C may be due to the similarity in the crystal structure and lattice parameters of the cubic defect spinel $ZnTiO_3$ and cubic inverse spinel Zn_2TiO_4 observed at the respective temperatures. These phase transitions are well supported by thermal analysis, powder XRD, EDAX, FT-IR and Raman spectroscopy. The optical bandgap was found to vary in the range of 3.59 eV to 3.84 eV with increase in calcination temperature.

Acknowledgments

The authors thank VIT-SIF for thermal analysis, powder XRD, FT-IR and DRS, and Dr. R.P. Vijayalakshmi, Sri Venkateswara University, Tirupati for Raman spectral data. One of the authors, B. Lokesh thanks VIT University for providing financial support to carry out the present work.

References

1. Pineda M, Fierro J L G, Palacios J M, Cilleruelo C, Garcia E and Ibarra J V 1997 *Appl. Surf. Sci.* **119** 1
2. Pal N, Paul M and Bhaumik A 2011 *Appl. Catal., A.* **393** 153
3. Wu S P, Luo J H and Cao S X 2010 *J. Alloys Compd.* **502** 147
4. Yadav B C, Yadav A, Singh S and Singh K 2013 *Sens. Actuators B.* **177** 605

5. Obayashi H, Sakurai Y and Gejo T 1976 *J. Solid State Chem.* **17** 299
6. Wang N, Li X, Wang Y, Hou Y, Zou X and Chen G 2008 *Mater. Lett.* **62** 3691
7. Darzi S J and Mahjoub A R 2009 *J. Alloys Compd.* **486** 805
8. McCord A T and Saunder H F 1945 U.S Patent 2379019
9. Steinike U and Wallis B 1997 *Cryst. Res. Technol.* **32** 187
10. Jain P K, Kumar D, Kumar A and Kaur D 2010 *Opto. Mater. Adv. Mater.* **4** 299
11. Manik S K and Pradhan S K 2006 *Physica E* **33** 69
12. Mrazek J, Spanhel L, Chadyron G and Matejec V 2010 *J. Phys. Chem. C.* **114** 2843
13. Hou L, Hou Y D, Zhu M K, Tang J, Liu J B, Wang H and Yan H 2005 *Mater. Lett.* **59** 197
14. Nolan N T, Seery M K and Pillai S C 2011 *Chem. Mater.* **23** 1496
15. Chai Y L, Chang Y S, Chen G J and Hsiao Y J 2008 *Mater. Res. Bull.* **43** 1066
16. Wang C L, Hwang W S, Chang K M, Ko H H, Hisn C S, Huang H H and Wang M C 2011 *Int. J. Mol. Sci.* **12** 935
17. Lee Y C and Chen P S 2013 *Thin Solid Films.* **531** 222
18. Ramirez E G, Chaparro M M and Angel O Z 2010 *Appl. Phys. A.* **108** 291
19. Phani A R, Passacantando M and Santucci S 2007 *J. Phys. Chem. Solids.* **68** 317
20. Liu X 2012 *Mater. Lett.* **80** 69
21. Liu Z, Zhou D, Gong S and Li H 2009 *J. Alloys Compd.* **475** 840
22. Kim H T, Kim S H, Nahm S and Byun J D 1999 *J. Am. Ceram. Soc.* **82** 3043
23. Cassaignon S, Koelsch M and Jolivet J P 2007 *J. Phys. Chem. Solids.* **68** 695
24. Svehla G 1979 In *Vogel's Text book of macro and semimicro Qualitative Inorganic Analysis* 5th edition (London and New York: Longman) p 272 and 532
25. Zhong S L, Xu R, Wang L, Li Y and Zhang L F 2011 *Mater. Res. Bull.* **46** 2385
26. Chamberland B L and Silverman S 1979 *J. Less. Common. Met.* **65** P41
27. Yuan Z, Huang F, Sun J and Zhou Y 2002 *Chem. Lett.* **31** 408
28. Sharma Y, Sharma N, Rao G V S and Chowdari B V R 2009 *J. Power Sources* **192** 627
29. Lu W and Schmidt H 2005 *J. Eur. Ceram. Soc.* **25** 919
30. Yang J and Swisher J H 1996 *Mater. Charact.* **37** 153
31. Wang C T and Lin J C2008 *Appl. Surf. Sci.* **254** 4500
32. Yamaguchi O, Morimi M, Kawabata H and Shimizu K 1987 *J. Am. Ceram. Soc.* **70** C-97
33. Li G, Li L, Goates J B and Woodfield B F 2009 *J. Am. Chem. Soc.* **127** 8659
34. Zheng M, Xing X., Deng J, Li L, Zhao J, Qiao L and Fang C 2007 *J. Alloys Compd.* **456** 353
35. Wang L, Kang H, Xue D and Liu C 2009 *J. Cryst. Growth.* **311** 611
36. Jeong T S, Han M S and Youn C J 2004 *J. Appl. Phys.* **96** 175
37. Wang Z, Saxena S K and Zha C S 2002 *Phys. Review B.* **66** 024103
38. Krylova G, Brioude A, Girard S A, Mrazek J and Spanhel L 2010 *Phys. Chem. Chem. Phys.* **12** 15101
39. Huo Y and Hu Y H 2012 *Ind. Eng. Chem. Res.* **51** 1083
40. Shi L and Lin H 2011 *Langmuir* **27** 3977